7. SYNTHESIS OF SERIES III

Chapter VII

7. Synthesis - Series III-Indole Thiazolidinedione hybrid analogues

7.1. Rationale

The previous chapter discussed about the role of carbon linker between indole and TZD pharmacophore in demonstrating PL inhibition. The study resulted in the synthesis of 28 hybrid analogues (Series II), wherein **6d** and **6e** were found to be most potent analogues with and IC_{50} value of 6.19 and 8.96 µM, respectively. Nevertheless, these analogues exhibited a lower PL inhibitory activity compared to the orlistat, that highlighted the need for further structural modification of the hybrid analogues.

Literature review revealed the potential role of π-cation interaction of Arg-256 in the PL inhibition. In order to achieve the active conformation for PL, the open lid structure requires an interaction of Arg 256 with the synthesized analogues [1–3]. Lack of this interaction results in a disruption of an optimal condition of lid domain amino acids. Thus, in the present structural modification, an attempt was made to increase the interaction with Arg256. Preliminary molecular docking implied that the distance between the aromatic functionalities and Arg 256 can be reduced by the addition of linker between them. This would provide additional conformational states for the analogues due to the flexible carbon linker. Further, numerous simple aromatic functionalities such as phenyl, indole and imidazole have been reported to possess π-cation interactions. Amongst these, indole was reported to possess the strongest π-cation interactions [4]. Hence, the phenyl ring was replaced with an indole functionality for stronger Arg256 interaction (**Fig. 7.1**).

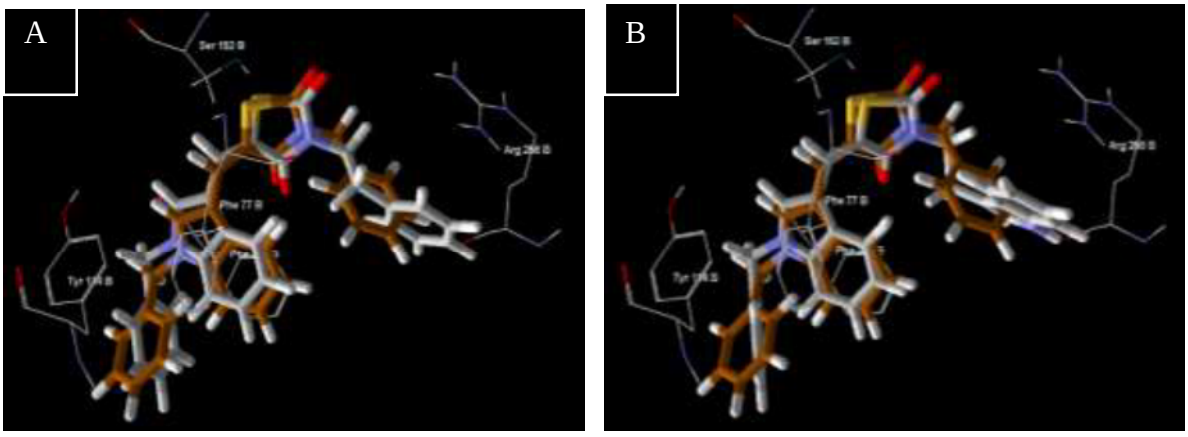

Fig. 7.1. Overlay diagram indicating the importance of linker extension and indole scaffold. **6d** (Brown); A- Extension of linker by phenyl and phenethyl functionality; B- Extension of linker by phenethyl and ethyl indole functionality

Additionally, it has been also observed that natural products with prenyl, and geranyl substituents exhibited potential PL inhibition (**Fig. 7.2**) [5,6]. Thus, the substitution of these functionalities in the hybrid analogues would cause an increment in their hydrophobicity. This in turn would increase the extent of interactions of these analogues with lid domain of the PL.

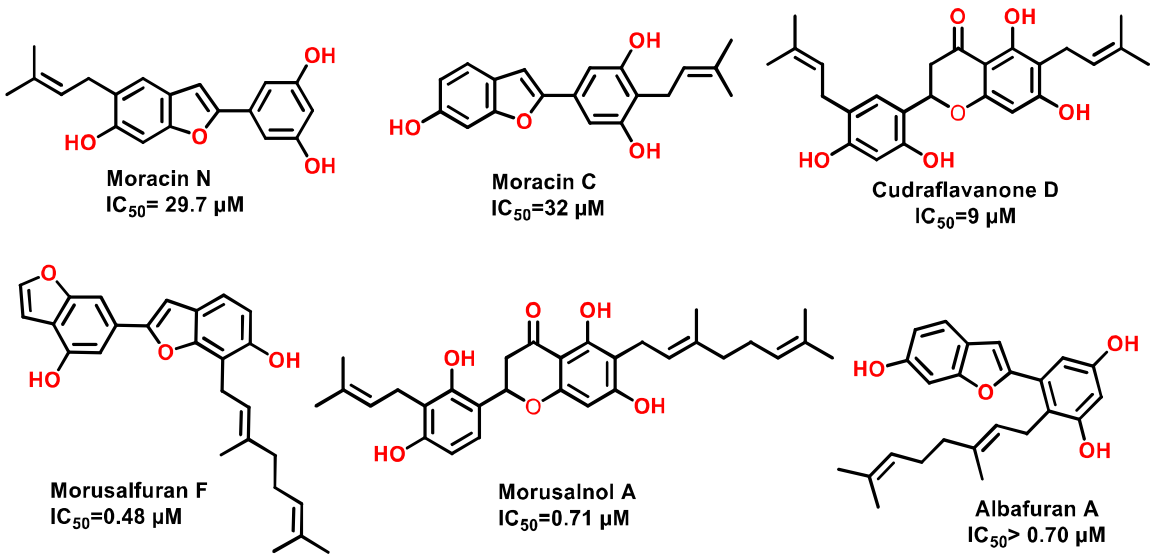

Fig. 7.2. Structures of prenyl/geranyl containing natural products.

The present chapter thus focussed on further structural optimization of the indole-TZD hybrid analogues (Series II) as discussed above (summarised as **Fig. 7.3**). The strategy aimed

i) to optimize the linker and substituents attached to the TZD scaffold for - cation interaction with Arg 256.

ii) to enhance the hydrophobicity on the indole nucleus *via* prenyl/ geranyl functionalities

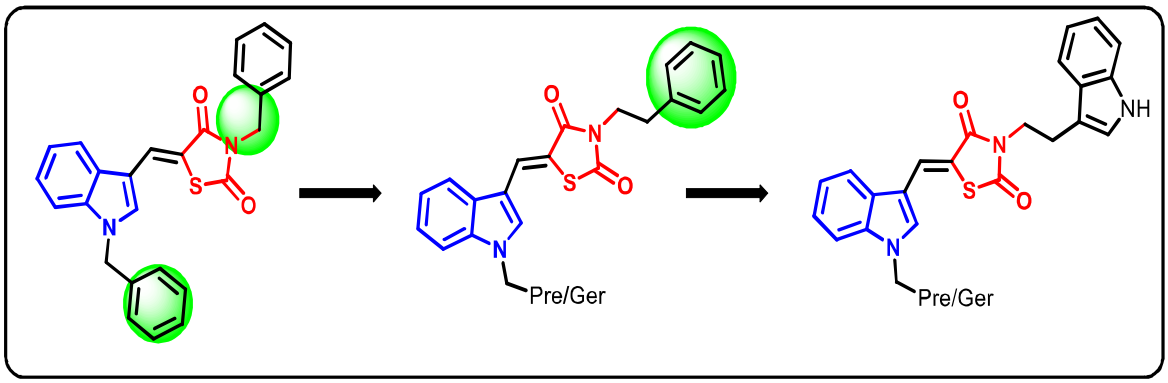

Fig. 7.3. Rationale for the designing of the hybrid analogues

7.2. Synthesis and Characterisation

The procedure for the syntheses of all the final analogues **7a** to **7u** were carried out as per the procedure detailed in Chapter 6, with minor modifications (**Scheme 7.1**). Briefly, condensation of thiourea (**1**) with chloroacetic acid (**2**) followed by refluxing with conc. HCl for 10-12 h resulted in the formation of 2,4-TZD (**3**) as white fine crystals [2]. *N* (3)-alkylation of TZDs was carried out by treating TZD with NaH followed by the addition of 2-phenylethyl bromide/ 3-(2-bromoethyl) indole [7]. After the specified time, the reaction mixture was poured into ice-cold water resulting in the formation of *N*-substituted 2,4-TZD (**4**). N-substitution of alkyl/aryl moieties on indole and its various benzyloxy derivatives were carried out in the presence NaH [8]. The obtained products were further proceeded for the synthesis of the respective Knoevenagel condensed hybrid analogues in ethanol, wherein TZD derivatives were treated with indole derivatives in the presence of glacial acetic and piperidine [2,9]

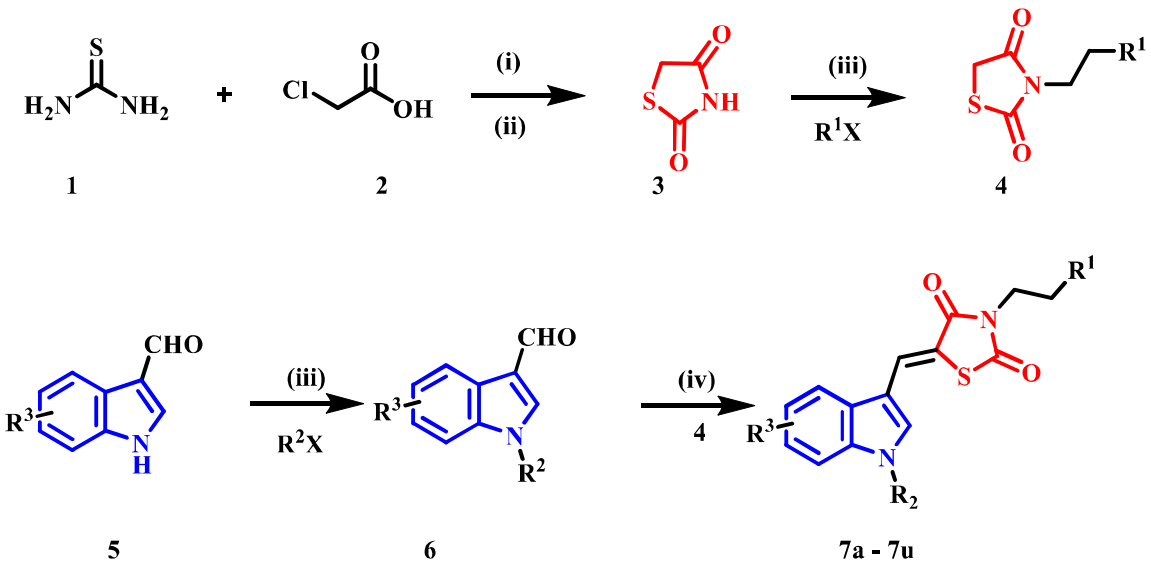

R^1-Benzyl or indolyl
R^2-H, Methyl, Ethyl, Benzyl, *P*-chlorobenzyl,*P*-bromobenzyl , *P*-nitrobenzyl, Prenyl, Geranyl
R^3-H or 4/5/7-benzyloxy

Scheme 7.1. Synthesis of series III analogues (7a- 7u). Reagents and conditions (i) 0-5°C, 30 min; (ii) HCl, H_2O, 110-120 °C, 10-12 h; (iii) NaH, DMF, overnight; (iv) Piperidine, Glacial acetic acid, EtOH, 6-8 h, Reflux

Characterisation

Reaction of various indole carboxaldehyde derivatives with TZD primarily involved the Knoevenagel condensation. The analogues (**7a to 7u**) were obtained in good yield with a buff yellowish colour and were characterised by ATIR, ^{1}H, ^{13}C NMR spectroscopy and

mass spectrometry HRMS [ESI mode]. The obtained data were similar to the previous chapter and in good agreement with their structural identity. The arylidene group proton appeared as singlet or multiplet at >8.16 δ ppm, indicating that the analogues predominantly formed were in "*Z*" configuration [10]. -CH_2 attached to the imidic nitrogen resonated at a value of 4.14 to 3.84 δ ppm, while -CH_2 neighbouring to the phenyl/indole resonated at 3.24 to 2.93 δ ppm. Terminal methyl groups of prenyl/geranyl resonated at 1.90-1.62 δ ppm. Further, the -CH_2 present in the benzyloxy functionality resonated at 5.37 to 5.17 δ ppm. Finally, the assigned structures of various analogues were confirmed by their mass spectra where characteristic $[M+H]^+$ peak was observed. Detailed information on characterisation of all the analogues are given below.

(Z)-5-((1H-Indol-3-yl)methylene)-3-phenethylthiazolidine-2,4-dione (7a)

Yield: 55%; Buff yellow solid; m.p: 231-232 °C; ^{1}H NMR (400 MHz, DMSO-d_6) δ 12.22 (s, 1H, -NH), 8.16 (s, 1H, -H of methylene), 7.90 (d, *J* = 7.8 Hz, 1H, H_7 of indole), 7.79 (d, *J* = 2.7 Hz, 1H, H_2 of indole), 7.52 (d, *J* = 8.0 Hz, 1H), 7.34 – 7.16 (m, 7H, aromatic), 3.93 – 3.84 (m, 2H,-CH_2 attached to imidic nitrogen), 2.93 (t, *J* = 7.4 Hz, 2H, -CH_2 attached to phenyl ring); ^{13}C NMR (100 MHz, DMSO-d_6) δ 167.35, 165.83, 138.33, 136.70, 129.49, 129.13, 128.94, 127.24, 127.00, 126.05, 123.61, 121.62, 118.84, 114.07, 112.92, 110.88, 42.94, 33.38; IR (ATR) υ; 3276, 3047, 2849, 2576, 2469, 2352, 1723, 1661, 1587, 1501, 1433, 1379, 1330, 1215, 1137, 982, 825, 735, 693, 648 cm^{-1}; HRMS (ESI$^+$) calculated for $C_{20}H_{16}N_2O_2S$ $[M+H]^+$, 349.0932; found 349.0952.

(Z)-5-((1-Methyl-1H-indol-3-yl)methylene)-3-phenethylthiazolidine-2,4-dione (7b)

Yield: 65%; Buff yellow solid; m.p: 226-227 °C; ^{1}H NMR (400 MHz, $CDCl_3$) δ 8.24 (d, *J* = 0.7 Hz, 1H, -H of methylene), 7.87 (dt, *J* = 7.8, 1.1 Hz, 1H, H_7 of indole), 7.41 – 7.24 (m, 9H, aromatic), 4.05 – 3.97 (m, 2H,-CH_2 attached to imidic nitrogen), 3.92 (s, 3H, -CH_3), 3.06 – 2.97 (m, 2H, -CH_2 attached to phenyl ring); ^{13}C NMR (100 MHz, $CDCl_3$) δ 167.46, 166.21, 137.71, 136.97, 131.21, 128.92, 128.62, 127.92, 126.74, 125.58, 123.66, 121.72, 118.91, 114.65, 110.96, 110.00, 42.99, 33.90, 33.70; IR (ATR) υ; 3781, 3357, 3108, 3016, 2914, 2531, 2356, 1715, 1655, 1587, 1447, 1383, 1329, 1225, 1123, 1054, 1001, 896, 730, 683 cm^{-1}; HRMS (ESI$^+$) calculated for $C_{21}H_{18}N_2O_2S$ $[M+H]^+$, 363.1089; found 363.1097.

(Z)-5-((1-Ethyl-1H-indol-3-yl)methylene)-3-phenethylthiazolidine-2,4-dione (7c)

Yield: 59%; Buff yellow solid; m.p: 156-157 °C; ^{1}H NMR (400 MHz, $CDCl_3$) δ 8.26 (d, *J* = 0.7 Hz, 1H, -H of methylene), 7.88 (dt, *J* = 7.6, 1.1 Hz, 1H, H_7 of indole), 7.49 – 7.22 (m, 9H, aromatic), 4.30 (q, *J* = 7.3 Hz, 2H, -CH_2 attached to indole ring), 4.06 – 3.97 (m, 2H,-CH_2 attached to imidic nitrogen), 3.07 – 2.98 (m, 2H, -CH_2 attached to phenyl ring), 1.58 (t, *J* = 7.3 Hz, 3H, -CH_3); ^{13}C NMR (100 MHz, $CDCl_3$) δ 167.48, 166.23, 137.71, 136.04, 129.58, 128.92, 128.62, 128.15, 126.74, 125.69, 123.54, 121.68, 119.03, 114.48, 111.06, 110.10, 43.00, 41.99, 33.90, 15.24; IR (ATR) υ; 3287, 3032, 2979, 2931, 2857, 2568, 2327, 1717, 1656, 1580, 1508, 1438, 1327, 1209, 1125, 1010, 908, 823, 735, 688 cm^{-1}; HRMS (ESI^+) calculated for $C_{22}H_{20}N_2O_2S$ $[M+H]^+$, 377.1245; found 377.1252.

(Z)-5-((1-Benzyl-1H-indol-3-yl)methylene)-3-phenethylthiazolidine-2,4-dione (7d)

Yield: 65%; Buff yellow solid; m.p: 162-163 °C; ^{1}H NMR (400 MHz, $CDCl_3$) δ 8.26 (s, 1H, -H of methylene), 7.94 – 7.85 (m, 1H, H_7 of indole), 7.45 (s, 1H, aromatic), 7.41 – 7.29 (m, 10H, aromatic), 7.27 – 7.18 (m, 3H, aromatic), 5.42 (s, 2H, -CH_2 attached to indole ring), 4.06 – 3.97 (m, 2H,-CH_2 attached to imidic nitrogen), 3.06 – 2.93 (m, 2H, -CH_2 attached to phenyl ring); ^{13}C NMR (100 MHz, $CDCl_3$) δ 167.41, 166.18, 137.67, 136.55, 135.65, 130.51, 129.10, 128.92, 128.62, 128.31, 128.15, 127.01, 126.75, 125.46, 123.81, 121.86, 119.04, 115.22, 111.52, 110.56, 51.01, 43.01, 33.89; IR (ATR) υ; 3458, 3390, 3091, 2936, 2512, 2367, 1727, 1672, 1599, 1520, 1449, 1381, 1336, 1242, 1170, 1017, 826, 743, 700, 656 cm^{-1}; HRMS (ESI^+) calculated for $C_{27}H_{22}N_2O_2S$ $[M+H]^+$, 439.1402; found 439.1398.

(Z)-5-((1-(4-Chlorobenzyl)-1H-indol-3-yl)methylene)-3-phenethylthiazolidine-2,4-dione (7e)

Yield: 65%; Buff yellow solid; m.p: 167-168 °C; ^{1}H NMR (400 MHz, $CDCl_3$) δ 8.25 (d, *J* = 0.7 Hz, 1H, -H of methylene), 7.89 (ddd, *J* = 6.7, 3.3, 2.1 Hz, 1H, H_7 of indole), 7.44 (d, *J* = 0.6 Hz, 1H, aromatic), 7.33 (dddd, *J* = 12.0, 6.7, 3.5, 1.5 Hz, 8H, aromatic), 7.28 – 7.24 (m, 2H, aromatic), 7.15 – 7.05 (m, 2H, aromatic), 5.40 (s, 2H, -CH_2 attached to indole ring), 4.06 – 3.97 (m, 2H,-CH_2 attached to imidic nitrogen), 3.06 – 2.97 (m, 2H, -CH_2 attached to phenyl ring); ^{13}C NMR (100 MHz, $CDCl_3$) δ 167.29, 166.14, 137.63, 136.37, 134.22, 130.26, 129.29, 128.91, 128.62, 128.20, 128.16, 126.76, 125.26, 123.96, 121.97, 119.14, 115.60, 111.76, 110.43, 50.38, 43.04, 33.87; IR (ATR) υ; 3852, 3743, 3674, 3613,

2357, 2175, 1675, 1521, 1462, 1348, 1187, 1142, 1095, 794, 747, 667 cm^{-1}; HRMS (ESI^+) calculated for $C_{27}H_{21}ClN_2O_2S$ $[M+H]^+$, 473.1012; found 473.1012.

(Z)-5-((1-(4-Bromobenzyl)-1H-indol-3-yl)methylene)-3-phenethylthiazolidine-2,4-dione (7f)

Yield: 62%; Buff yellow solid; m.p: 176-177 °C; ^1H NMR (400 MHz, $CDCl_3$) δ 8.25 (s, 1H, -H of methylene), 7.90 (dd, J = 6.2, 3.0 Hz, 1H, H_7 of indole), 7.52 – 7.42 (m, 3H, aromatic), 7.38 – 7.24 (m, 9H, aromatic), 7.05 (d, J = 8.0 Hz, 2H, aromatic), 5.38 (s, 2H, -CH_2 attached to indole ring), 4.02 (t, J = 7.8 Hz, 2H,-CH_2 attached to imidic nitrogen), 3.02 (t, J = 7.7 Hz, 2H, -CH_2 attached to phenyl ring); ^{13}C NMR (100 MHz, $CDCl_3$) δ 167.29, 166.23, 137.64, 136.36, 134.78, 132.25, 130.28, 128.91, 128.63, 128.50, 128.16, 126.77, 125.24, 123.97, 122.26, 121.99, 119.15, 115.66, 111.78, 110.44, 50.43, 43.04, 33.88; IR (ATR) υ; 3352, 3023, 2930, 2356, 1730, 1667, 1602, 1469, 1427, 1346, 1234, 1180, 1132, 1078, 1008, 946, 834, 787, 739, 661 cm^{-1}; HRMS (ESI^+) calculated for $C_{27}H_{21}BrN_2O_2S$ $[M+H]^+$, 517.0507; found 517.0490.

(Z)-5-((1-(4-Nitrobenzyl)-1H-indol-3-yl)methylene)-3-phenethylthiazolidine-2,4-dione (7g)

Yield: 53%; Buff yellow solid; m.p: 193-194 °C; ^1H NMR (400 MHz, $CDCl_3$) δ 8.28 – 8.17 (m, 3H, aromatic), 7.97 – 7.87 (m, 1H, aromatic), 7.48 (s, 1H, aromatic), 7.38 – 7.29 (m, 7H, aromatic), 7.28 – 7.22 (m, 3H, aromatic), 5.55 (s, 2H, -CH_2 attached to indole ring), 4.06 – 3.98 (m, 2H,-CH_2 attached to imidic nitrogen), 3.02 (dd, *J* = 8.7, 6.8 Hz, 2H, -CH_2 attached to phenyl ring); ^{13}C NMR (100 MHz, $CDCl_3$) δ 167.10, 166.07, 147.83, 143.08, 137.58, 136.23, 130.06, 128.90, 128.63, 128.17, 127.37, 126.79, 124.92, 124.35, 124.27, 122.21, 119.36, 116.27, 112.26, 110.19, 50.29, 43.08, 33.86; IR (ATR) υ; 3392, 3238, 3094, 2930, 2854, 2514, 2356, 1722, 1662, 1598, 1517, 1439, 1334, 1231, 1167, 1132, 1010, 845, 737, 702 cm^{-1}; HRMS (ESI^+) calculated for $C_{27}H_{21}N_3O_4S$ $[M+H]^+$, 484.1253; found 484.1264.

(Z)-5-((1-(3-Methylbut-2-en-1-yl)-1H-indol-3-yl)methylene)-3-phenethylthiazolidine-2,4-dione (7h)

Yield: 59 %; Buff yellow solid; m.p: 142-143 °C; ^1H NMR (400 MHz, $CDCl_3$) δ 8.25 (s, 1H, -H of methylene), 7.87 (dd, *J* = 7.2, 1.4 Hz, 1H, -H_2 of indole), 7.46 – 7.24 (m, 10H, aromatic), 5.44 (tdd, *J* = 6.9, 2.9, 1.5 Hz, 1H, -H of prenyl), 4.79 (d, *J* = 7.0 Hz, 2H, -CH_2 attached to indole ring), 4.06 – 3.97 (m, 2H,-CH_2 attached to imidic nitrogen), 3.06 – 2.98

(m, 2H, -CH_2 attached to phenyl ring), 1.87 (dd, *J* = 14.6, 1.4 Hz, 6H, 2 -CH_3); ^{13}C NMR (100 MHz, $CDCl_3$) δ 167.57, 166.24, 138.63, 137.72, 136.33, 129.94, 128.92, 128.61, 128.24, 126.73, 125.78, 123.48, 121.71, 118.94, 118.20, 114.35, 110.94, 110.35, 44.93, 42.98, 33.90, 25.70, 18.22; IR (ATR) υ; 3852, 3743, 3674, 3614, 3104, 2818, 2357, 2175, 2113, 1917, 1687, 1520, 1463, 1189, 1142, 794, 671 cm^{-1}; HRMS (ESI^+) calculated for $C_{25}H_{24}N_2O_2S$ $[M+H]^+$, 417.1558; found 417.1563.

(Z)-5-((1-((E)-3,7-Dimethylocta-2,6-dien-1-yl)-1H-indol-3-yl)methylene)-3-phenethyl thiazolidine-2,4-dione (7i)

Yield: 53%; Buff yellow solid; m.p: 162-163 °C; ^{1}H NMR (400 MHz, $CDCl_3$) δ 8.25 (s, 1H), 7.91 – 7.84 (m, 1H, -H of methylene), 7.42 (d, *J* = 19.0 Hz, 2H, aromatic), 7.38 – 7.21 (m, 7H, aromatic), 5.44 (dt, *J* = 6.6, 4.2 Hz, 1H, -H of geranyl), 5.10 (dh, *J* = 6.9, 1.8 Hz, 1H), 4.81 (d, *J* = 6.9 Hz, 2H, -CH_2 attached to indole ring), 4.06 – 3.97 (m, 2H, -CH_2 attached to imidic nitrogen), 3.06 – 2.97 (m, 2H, -CH_2 attached to indole ring), 2.16 (d, *J* = 5.3 Hz, 4H, -CH_2 of geranyl), 1.88 (d, *J* = 1.3 Hz, 3H, -CH_3 of geranyl), 1.62 (s, 4H); ^{13}C NMR (100 MHz, $CDCl_3$) δ 167.53, 166.24, 142.10, 137.71, 136.35, 132.18, 129.96, 128.92, 128.61, 128.24, 126.73, 125.79, 123.47, 123.40, 121.71, 118.92, 118.03, 114.34, 110.92, 110.40, 44.92, 42.98, 39.45, 33.90, 26.32, 25.68, 17.76, 16.64; IR (ATR) υ; 3851, 3743, 3673, 3613, 3389, 2822, 2357, 2175, 1665, 1519, 1459, 1352, 1263, 1212, 1018, 793 cm^{-1}; HRMS (ESI^+) calculated for $C_{30}H_{32}N_2O_2S$ $[M+H]^+$, 485.2184; found 485.2185.

(Z)-3-(2-(1H-Indol-3-yl)ethyl)-5-((1H-indol-3-yl)methylene)thiazolidine-2,4-dione (7j)

Yield: 45%; Buff yellow solid; m.p: 154-155 °C; ^{1}H NMR (400 MHz, DMSO-d_6) δ 12.02 (s, 1H), 8.16 (s, 1H, -H of methylene), 7.90 (d, *J* = 7.8 Hz, 1H, aromatic), 7.79 (d, *J* = 2.7 Hz, 1H, aromatic), 7.52 (d, *J* = 8.0 Hz, 1H), 7.34 – 7.16 (m, 8H, aromatic), 3.93 – 3.84 (m, 2H, -CH_2 attached to imidic nitrogen), 2.93 (t, *J* = 7.4 Hz, 2H, -CH_2 attached to indole); ^{13}C NMR (100 MHz, DMSO-d_6) δ 166.35, 165.43, 138.13, 136.70, 131.08, 129.79, 129.68, 129.23, 128.94, 127.24, 127.00, 126.05, 123.61, 122.20, 121.62, 119.64, 118.84, 114.07, 112.92, 110.88, 42.94, 33.38; IR (ATR) υ; 3853, 3748, 3611, 3309, 2969, 2875, 2811, 2357, 1736, 1668, 1521, 1459, 1383, 1338, 1229, 1142, 1094, 996, 741, 671 cm^{-1}; HRMS (ESI^+) calculated for $C_{22}H_{17}N_3O_2S$ $[M+H]^+$, 388.1041; found 388.1048.

(Z)-3-(2-(1H-Indol-3-yl)ethyl)-5-((1-methyl-1H-indol-3-yl)methylene)thiazolidine-2,4-dione (7k)

Yield: 59%; Buff yellow solid; m.p: 249-250 °C; ^{1}H NMR (400 MHz, $CDCl_3$) δ 8.27 (d, *J* = 0.7 Hz, 1H, -H of methylene), 8.04 (s, 1H, aromatic), 7.84 (ddt, *J* = 29.1, 7.7, 0.9 Hz, 2H, aromatic), 7.44 – 7.31 (m, 4H, aromatic), 7.26 – 7.13 (m, 3H, aromatic), 4.14 – 4.05 (m, 2H,-CH_2 attached to imidic nitrogen), 3.93 (s, 3H,-CH_3), 3.24 – 3.15 (m, 2H, -CH_2 attached to indole ring); ^{13}C NMR (100 MHz, $CDCl_3$) δ 167.63, 166.43, 136.98, 136.24, 131.18, 127.94, 127.41, 125.51, 123.64, 122.20, 122.12, 121.70, 119.64, 118.91, 114.89, 112.16, 111.10, 111.00, 109.99, 42.32, 33.72, 23.77; IR (ATR) υ; 3852, 3746, 3612, 3419, 2357, 1718, 1670, 1600, 1520, 1460, 1230, 1129, 1073, 998, 912, 837, 729 cm^{-1}; HRMS (ESI^+) calculated for $C_{23}H_{19}N_3O_2S$ $[M+H]^+$, 402.1198; found 402.1199.

(Z)-3-(2-(1H-indol-3-yl)ethyl)-5-((1-ethyl-1H-indol-3-yl)methylene)thiazolidine-2,4-dione (7l)

Yield: 55%; Buff yellow solid; m.p: 210-211 °C; ^{1}H NMR (400 MHz, $CDCl_3$) δ 8.28 (d, *J* = 0.7 Hz, 1H, -H of methylene), 8.07 (s, 1H, aromatic), 7.92 – 7.78 (m, 2H, aromatic), 7.50 – 7.28 (m, 5H, aromatic), 7.28 – 7.10 (m, 3H, aromatic), 4.29 (q, *J* = 7.3 Hz, 2H, -CH_2 attached to indole ring), 4.14 – 4.06 (m, 2H,-CH_2 attached to imidic nitrogen), 3.24 – 3.15 (m, 2H, -CH_2 attached to indole ring), 1.58 (t, *J* = 7.3 Hz, 3H, -CH_2); ^{13}C NMR (100 MHz, $CDCl_3$) δ 167.66, 166.45, 136.26, 136.04, 129.57, 128.16, 127.42, 125.61, 123.52, 122.19, 122.15, 121.67, 119.63, 119.03, 118.92, 114.71, 112.14, 111.12, 111.09, 110.10, 42.32, 41.99, 23.78, 15.23; IR (ATR) υ; 3851, 3744, 3673, 3613, 3368, 2818, 2357, 1718, 1662, 1589, 1519, 1460, 1381, 1333, 1215, 1137, 1084, 995, 839, 733 cm^{-1}; HRMS (ESI^+) calculated for $C_{24}H_{21}N_3O_2S$ $[M+H]^+$, 416.1354; found 416.1346.

(Z)-3-(2-(1H-Indol-3-yl)ethyl)-5-((1-benzyl-1H-indol-3-yl)methylene)thiazolidine-2,4-dione (7m)

Yield: 65%; Buff yellow solid; m.p: 233-234 °C; ^{1}H NMR (400 MHz, DMSO-d_6) δ 10.91 – 10.85 (m, 1H, -NH of indole), 8.19 (s, 1H, -H of methylene), 8.08 (s, 1H, aromatic), 8.00 – 7.92 (m, 1H, aromatic), 7.64 – 7.54 (m, 2H, aromatic), 7.39 – 7.19 (m, 9H, aromatic), 7.13 – 6.97 (m, 2H, aromatic), 5.61 (s, 2H, -CH_2 attached to indole ring), 3.93 (t, *J* = 7.7 Hz, 2H,-CH_2 attached to imidic nitrogen), 3.05 (t, *J* = 7.6 Hz, 2H, -CH_2 attached to indole ring); ^{13}C NMR (100 MHz, DMSO-d_6) δ 167.47, 165.97, 137.53, 136.73, 136.51, 132.34, 129.16, 128.17, 128.04, 127.71, 127.54, 125.31, 123.82, 123.54, 122.01, 121.53, 119.26, 118.91, 118.48, 114.89, 111.96, 111.81, 110.69, 110.55, 50.25, 42.50, 23.63; IR (ATR) υ; 3850, 3744, 3674, 3614, 3431, 2588, 2357, 2176, 1674, 1603, 1522, 1459, 1353, 1246,

1187, 1143, 1020, 970, 745, 669 cm^{-1}; HRMS (ESI^+) calculated for $C_{29}H_{23}N_3O_2S$ $[M+H]^+$, 478.1511; found 478.1536.

(Z)-3-(2-(1H-Indol-3-yl)ethyl)-5-((1-(4-chlorobenzyl)-1H-indol-3-yl)methylene) thiazolidine-2,4-dione (7n)

Yield: 59%; Buff yellow solid; m.p: 198-199°C; ; ^1H NMR (400 MHz, $CDCl_3$) δ 8.28 (s, 1H, , -H of methylene), 8.06 (s, 1H, aromatic, , aromatic), 7.93 – 7.86 (m, 1H, , aromatic), 7.80 (d, *J* = 7.7 Hz, 1H, , aromatic), 7.47 – 7.31 (m, 8H, aromatic), 7.19 – 7.07 (m, 4H, aromatic), 5.40 (s, 2H, -CH_2 attached to indole ring), 4.10 (t, *J* = 7.9 Hz, 2H, -CH_2 attached to imidic nitrogen), 3.19 (t, *J* = 7.9 Hz, 2H, -CH_2 attached to indole ring); ^{13}C NMR (100 MHz, $CDCl_3$) δ 167.46, 166.35, 136.38, 136.26, 134.26, 134.20, 130.27, 129.29, 128.20, 127.40, 125.18, 123.94, 122.21, 122.15, 121.97, 119.65, 119.15, 118.90, 118.63, 115.83, 112.09, 111.79, 111.13, 110.44, 50.37, 42.35, 23.76; IR (ATR) υ; 3851, 3744, 3674, 3614, 3109, 2516, 2516, 2357, 2175, 2114, 1917, 1695, 1521, 1464, 1395, 1342, 794, 749, 670 cm^{-1}; HRMS (ESI^+) calculated for $C_{29}H_{22}ClN_3O_2S$ $[M+H]^+$, 511.1121; found 512.1101.

(***Z)-3-(2-(1H-Indol-3-yl)ethyl)-5-((1-(4-bromobenzyl)-1H-indol-3-yl)methylene) thiazolidine -2,4-dione (7o)***

Yield: 58%; Buff yellow solid; m.p: 155-157 °C; ^1H NMR (400 MHz, $CDCl_3$) δ 8.27 (s, 1H, -H of methylene), 8.06 (s, 1H, aromatic), 7.94 – 7.85 (m, 1H, aromatic), 7.84 – 7.77 (m, 1H, aromatic), 7.54 – 7.30 (m, 6H, aromatic), 7.29 – 7.01 (m, 5H, aromatic), 5.37 (s, 2H, -CH_2 attached to indole ring), 4.14 – 4.05 (m, 2H, -CH_2 attached to imidic nitrogen), 3.23 – 3.14 (m, 2H, -CH_2 attached to indole ring); ^{13}C NMR (100 MHz, $CDCl_3$) δ 167.45, 166.34, 136.36, 136.25, 134.80, 132.24, 130.27, 128.48, 128.17, 127.40, 125.16, 123.95, 122.24, 122.20, 122.15, 121.97, 119.64, 119.14, 118.89, 115.85, 112.07, 111.80, 111.13, 110.44, 50.41, 42.35, 23.76; IR (ATR) υ; 3851, 3743, 3673, 3614, 2586, 2357, 2175, 2114, 1917, 1683, 1521, 1463, 1394, 1349, 1188, 1140, 1013, 794, 750, 668 cm^{-1}; HRMS (ESI^+) calculated for $C_{29}H_{22}BrN_3O_2S$ $[M+H]^+$, 555.0616; found 556.0692.

(Z)-3-(2-(1H-Indol-3-yl)ethyl)-5-((1-(4-nitrobenzyl)-1H-indol-3-yl)methylene) thiazolidine -2,4-dione (7p)

Yield: 50%; Buff yellow solid; m.p: 193-194 °C; ^1H NMR (400 MHz, $CDCl_3$) δ 8.33 – 8.18 (m, 4H, aromatic), 8.12 (d, *J* = 9.2 Hz, 0H, aromatic), 8.08 (d, *J* = 5.9 Hz, 1H, aromatic), 7.96 – 7.88 (m, 1H, aromatic), 7.79 (d, *J* = 7.6 Hz, 1H, aromatic), 7.48 (s, 1H,

aromatic), 7.43 – 7.07 (m, 12H, aromatic), 5.54 (s, 2H, -CH_2 attached to indole ring), 4.14 – 4.05 (m, 2H,-CH_2 attached to imidic nitrogen), 3.19 (t, *J* = 7.9 Hz, 2H, -CH_2 attached to indole ring); ^{13}C NMR (100 MHz, $CDCl_3$) δ 167.27, 166.28, 147.82, 143.11, 136.25, 130.06, 129.65, 128.18, 127.54, 127.36, 124.84, 124.47, 124.35, 124.25, 122.22, 122.16, 119.65, 119.36, 118.86, 116.49, 112.29, 112.03, 111.15, 110.19, 50.28, 42.40, 23.74; IR (ATR) υ; 3851, 3744, 3674, 3614, 3109, 2516, 2516, 2357, 2175, 2114, 1917, 1695, 1521, 1464, 1395, 1342, 794, 749, 670 cm^{-1}; HRMS (ESI^+) calculated for $C_{29}H_{22}N_4O_4S$ $[M+H]^+$, 523.1362; found 523.1344.

(Z)-3-(2-(1H-Indol-3-yl)ethyl)-5-((1-(3-methylbut-2-en-1-yl)-1H-indol-3-yl)methylene) thiazolidine-2,4-dione (7q)

Yield: 59%; Buff yellow solid; m.p: 166-167 °C; ^{1}H NMR (400 MHz, $CDCl_3$) δ 8.28 (s, 1H, -H of methylene), 8.06 (s, 1H, aromatic), 7.88 (d, *J* = 7.7 Hz, 1H, , aromatic), 7.81 (d, *J* = 7.7 Hz, 1H, aromatic), 7.48 – 7.26 (m, 6H, aromatic), 7.26 – 7.11 (m, 3H, aromatic), 5.45 (t, *J* = 7.1 Hz, 1H, -CH of prenyl), 4.80 (d, *J* = 7.0 Hz, 2H, -CH_2 attached to indole), 4.10 (t, *J* = 7.9 Hz, 2H, -CH_2 attached to imidic nitrogen), 3.20 (t, *J* = 7.9 Hz, 2H, -CH_2 attached to indole ring), 1.90 (s, 6H, -CH_3 of prenyl). ^{13}C NMR (100 MHz, $CDCl_3$) δ 167.74, 166.45, 138.60, 136.33, 136.25, 129.93, 128.26, 127.42, 125.71, 123.46, 122.19, 122.14, 121.70, 119.63, 118.94, 118.22, 114.59, 112.16, 111.11, 110.98, 110.35, 44.94, 42.30, 25.70, 23.78, 18.23; IR (ATR) υ; 3852, 3743, 3674, 3614, 3104, 2818, 2357, 2175, 2113, 1917, 1687, 1520, 1463, 1189, 1142, 794, 671 cm^{-1}; HRMS (ESI^+) calculated for $C_{27}H_{25}N_3O_2S$ $[M+H]^+$, 456.1667; found 455.1658.

(Z)-3-(2-(1H-Indol-3-yl)ethyl)-5-((1-((E)-3,7-dimethylocta-2,6-dien-1-yl)-1H-indol-3-yl)methylene)thiazolidine-2,4-dione (7r)

Yield: 55%; Buff yellow solid; m.p: 147-148 °C; ^{1}H NMR (400 MHz, $CDCl_3$) δ 8.26 (s, 1H, -H of methylene), 7.91 – 7.84 (m, 1H, aromatic), 7.47 – 7.22 (m, 10H, aromatic), 5.44 (tt, *J* = 5.5, 3.2 Hz, 1H, -CH of geranyl), 5.20-5.10 (m, 3H, -CH of geranyl), 4.81 (d, *J* = 6.9 Hz, 2H, -CH_2 attached to indole ring), 4.06 – 3.97 (m, 2H, -CH_2 attached to imidic nitrogen), 3.06 – 2.98 (m, 2H, -CH_2 attached to indole ring), 2.17 (d, *J* = 5.3 Hz, 4H, -CH_2 of geranyl), 1.88 (d, *J* = 1.3 Hz, 3H, -CH_3 of geranyl), 1.62 (d, *J* = 1.3 Hz, 6H, -CH_3 of geranyl); ^{13}C NMR (100 MHz, $CDCl_3$) δ 167.52, 166.24, 142.11, 137.72, 136.36, 132.18, 129.96, 128.92, 128.61, 128.24, 126.73, 125.78, 123.47, 123.41, 121.71, 118.93, 118.03, 114.36, 110.93, 110.40, 44.92, 42.98, 39.45, 33.90, 26.33, 25.68, 17.76, 16.64; IR (ATR)

υ; 3851, 3743, 3674, 3613, 3104, 2589, 2357, 2175, 2113, 1917, 1696, 1652, 1521, 1464, 794, 672 cm^{-1}; HRMS (ESI^+) calculated for $C_{32}H_{33}N_3O_2S$ $[M+H]^+$, 524.2293; found 524.2299.

(Z)-3-(2-(1H-Indol-3-yl)ethyl)-5-((4-(benzyloxy)-1-((E)-3,7-dimethylocta-2,6-dien-1-yl)-1H-indol-3-yl)methylene)thiazolidine-2,4-dione (7s)

Yield: 53%; Buff yellow solid; m.p: 188-189°C; ^1H NMR (400 MHz, $CDCl_3$) δ 9.01 (s, 1H, NH of indole), 8.04 (s, 1H, -H of methylene), 7.88 – 7.81 (m, 1H, aromatic), 7.61 (d, *J* = 7.6 Hz, 2H, aromatic), 7.48 (t, *J* = 7.5 Hz, 2H, aromatic), 7.38 (q, *J* = 5.2, 3.7 Hz, 3H, aromatic), 7.31 – 7.16 (m, 4H, aromatic), 7.12 (d, *J* = 1.9 Hz, 1H, aromatic), 7.02 (d, *J* = 8.2 Hz, 1H, aromatic), 6.75 (d, *J* = 7.8 Hz, 1H, aromatic), 5.44 (s, 1H, -CH of geranyl), 5.37 (s, 2H, $-CH_2$ attached to oxygen), 5.14 – 5.06 (m, 1H, -CH of geranyl), 4.76 (d, *J* = 6.9 Hz, 2H, $-CH_2$ attached to indole ring), 4.13 – 4.04 (m, 2H, $-CH_2$ attached to imidic nitrogen), 3.22 – 3.13 (m, 2H, $-CH_2$ attached to indole ring), 2.16 (q, *J* = 4.7, 3.9 Hz, 4H, $-CH_2$ of geranyl), 1.87 (d, *J* = 3.2 Hz, 3H, $-CH_3$ of geranyl), 1.69 (s, 3H, $-CH_3$ of geranyl), 1.63 (s, 3H, $-CH_3$ of geranyl); ^{13}C NMR (100 MHz, $CDCl_3$) δ 168.06, 166.24, 154.09, 142.00, 138.02, 136.98, 136.25, 132.16, 129.49, 128.98, 128.73, 128.69, 127.80, 127.45, 126.85, 126.81, 124.07, 123.45, 122.15, 122.12, 119.57, 119.05, 118.11, 117.64, 114.18, 112.29, 111.59, 111.10, 103.68, 103.47, 70.03, 45.05, 42.12, 39.46, 26.36, 25.71, 23.82, 17.79, 16.65; IR (ATR) υ; 3851, 3743, 3673, 3613, 3389, 2822, 2357, 2175, 1665, 1519, 1459, 1352, 1263, 1212, 1018, 793 cm^{-1}; HRMS (ESI^+) calculated for $C_{39}H_{39}N_3O_3S$ $[M+H]^+$, 630.2712; found 630.2677.

(Z)-3-(2-(1H-Indol-3-yl)ethyl)-5-((5-(benzyloxy)-1-((E)-3,7-dimethylocta-2,6-dien-1-yl)-1H-indol-3-yl)methylene)thiazolidine-2,4-dione (7t)

Yield: 55%; Buff yellow solid; m.p: 139-140 °C; ^1H NMR (400 MHz, $CDCl_3$) δ 8.23 (s, 1H, -H of methylene), 8.07 (s, 1H, aromatic), 7.82 (d, *J* = 7.6 Hz, 1H, aromatic), 7.53 (d, *J* = 7.0 Hz, 2H, aromatic), 7.49 – 7.27 (m, 8H, aromatic), 7.27 – 7.03 (m, 4H, aromatic), 5.17 (s, 2H, -CH of geranyl), 5.10 (qd, *J* = 5.2, 4.5, 2.0 Hz, 1H), 4.77 (d, *J* = 6.9 Hz, 2H, $-CH_2$ attached to indole ring), 4.14 – 4.05 (m, 2H, $-CH_2$ attached to imidic nitrogen), 3.23 – 3.14 (m, 2H, $-CH_2$ attached to indole ring), 2.16 (d, *J* = 5.6 Hz, 4H, $-CH_2$ of geranyl), 1.90 – 1.84 (m, 3H, $-CH_3$ of geranyl), 1.66 (d, *J* = 26.2 Hz, 6H, $-CH_3$ of geranyl); ^{13}C NMR (100 MHz, $CDCl_3$) δ 167.73, 166.53, 154.94, 142.07, 137.14, 136.24, 132.19, 131.56, 130.25, 128.97, 128.62, 127.97, 127.58, 127.41, 125.80, 123.42, 122.19, 122.15, 119.63, 118.93,

118.06, 114.55, 113.83, 112.15, 111.38, 111.13, 110.63, 101.79, 70.77, 45.14, 42.29, 39.45, 26.33, 25.72, 23.79, 17.79, 16.65; IR (ATR) υ; 3852, 3742, 3673, 3613, 2357, 2175, 1696, 1521, 1208, 1135, 794, 672 cm^{-1}; HRMS (ESI^+) calculated for $C_{39}H_{39}N_3O_3S$ $[M+H]^+$, 630.2712; found 630.2673.

(Z)-3-(2-(1H-Indol-3-yl)ethyl)-5-((7-(benzyloxy)-1-((E)-3,7-dimethylocta-2,6-dien-1-yl)-1H-indol-3-yl)methylene)thiazolidine-2,4-dione (7u)

Yield: 58%; Buff yellow solid; m.p: 125-126 °C; ^1H NMR (400 MHz, $CDCl_3$) δ 8.24 (s, 1H, -H of methylene), 8.05 (s, 1H, aromatic), 7.81 (d, *J* = 7.7 Hz, 1H, aromatic), 7.51 – 7.35 (m, 8H, aromatic), 7.27 – 7.10 (m, 4H, aromatic), 6.84 (d, *J* = 7.8 Hz, 1H, aromatic), 5.45 (t, *J* = 6.8 Hz, 1H, -CH of geranyl), 5.24 (s, 2H, $-CH_2$ attached to oxygen), 5.10 (t, *J* = 5.5 Hz, 3H, geranyl), 4.13 – 4.04 (m, 2H, $-CH_2$ attached to imidic nitrogen), 3.18 (dd, *J* = 9.3, 6.5 Hz, 2H, $-CH_2$ attached to indole ring), 2.15 – 2.02 (m, 4H, $-CH_2$ of geranyl), 1.65 (d, *J* = 35.1 Hz, 9H, $-CH_3$ of geranyl); ^{13}C NMR (100 MHz, $CDCl_3$) δ 167.76, 166.43, 146.98, 140.60, 136.60, 136.23, 132.00, 130.71, 128.73, 128.68, 128.17, 127.94, 127.60, 127.40, 126.23, 126.10, 125.90, 123.62, 122.24, 122.18, 122.15, 120.02, 119.63, 118.94, 114.47, 112.15, 111.56, 111.12, 111.08, 105.49, 70.62, 47.72, 42.27, 39.43, 26.46, 25.69, 23.79, 17.76, 16.51; IR (ATR) υ; 3851, 3743, 3674, 3613, 3104, 2589, 2357, 2175, 2113, 1917, 1696, 1652, 1521, 1464, 794, 672 cm^{-1}; HRMS (ESI^+) calculated for $C_{39}H_{39}N_3O_3S$ $[M+H]^+$, 630.2712; found 630.2680.

7.3. PL inhibition assay, enzyme kinetics and structural activity relationship

The *in-vitro* PL inhibitory activity of the synthesized analogues were evaluated by a standardised assay protocol [2,11]. As summarised in **Table 7.1**, the synthesized analogues displayed potential to moderate PL inhibition (IC_{50} = 2.67 to 18.64 µM). Amongst the benzyl substituted analogue, **7d** exhibited an activity of 5.01 µM. Further, replacement of aromatic moiety with alkyl chain resulted in the reduction of the PL inhibition (**7i;** IC_{50} = 4.59 µM). Substitution of denser groups (indole) in place of phenyl scaffold resulted in **7j-7r**, that exhibited a higher potential than the latter. Amongst these analogues, **7r** resulted in the potent activity of 2.67 µM. Incorporation of additional bulkiness on the indole scaffold resulted in the weakening of PL inhibition (**7s – 7u**).

Table 7.1 *In-vitro* PL inhibitory activity of the synthesized analogues (7a- 7u)

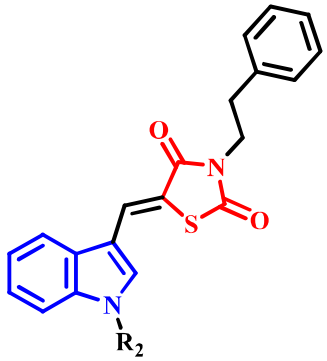

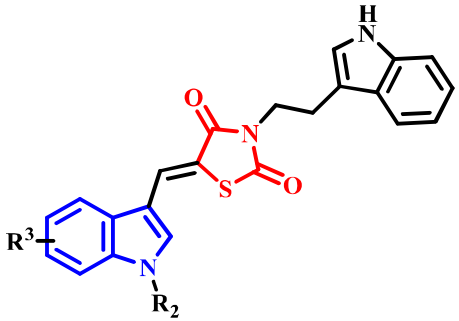

#	R^2	IC_{50} (µM) *	#	R^2	R^3	IC_{50} (µM) *
7a	H	18.64 ± 0.45	7j	H	H	17.25 ± 0.91
7b	Methyl	10.74 ± 0.37	7k	Methyl	H	10.68 ± 0.97
7c	Ethyl	12.20 ± 1.38	7l	Ethyl	H	10.56 ± 1.06
7d	**Benzyl**	**5.01 ± 0.84**	**7m**	**Benzyl**	**H**	**4.22 ± 0.58**
7e	4-Chlorobenzyl	10.83 ± 1.03	7n	4-Chlorobenzyl	H	8.32 ± 1.14
7f	4-Bromobenzyl	14.23 ± 0.24	7o	4-Bromobenzyl	H	10.65 ± 0.62
7g	4-Nitrobenzyl	18.11 ± 2.50	7p	4-Nitrobenzyl	H	12.76 ±1.80
7h	Prenyl	7.45 ± 1.17	7q	Prenyl	H	4.52 ± 0.40
7i	**Geranyl**	**4.59 ± 0.22**	**7r**	**Geranyl**	**H**	**2.67 ± 0.32**
			7s	Geranyl	4-benzyloxyl	5.14 ± 0.30
			7t	Geranyl	5-benzyloxyl	5.71 ± 0.50
			7u	Geranyl	7-benzyloxyl	16.84 ± 1.80

* All the experiments were performed in triplicate and the values are represented as mean ± S.E.M

The inhibition mode of the topmost active analogues (**7r** and **7m**) was evaluated by performing enzyme inhibition kinetic experiment (See chapter 3). The obtained LB plots converged at its first quadrant and intersected at one point, that indicated the analogues **7r** and **7m** exerted inhibition in a competitive manner (**Fig. 7.4**). A proportionate increase in the apparent K_m values without affecting the V_{max} further indicated a reversible competitive inhibition (**Table 7.2**). Inhibition constant (K_i) values were deduced as 1.483 and 2.924 µM (retrieved from the Cheng-Prusoff equation [12]), proving that these molecules have a strong affinity towards PL. From the enzyme kinetics study, it was concluded that the synthesized analogues were bound to the active site of the PL during the inhibition.

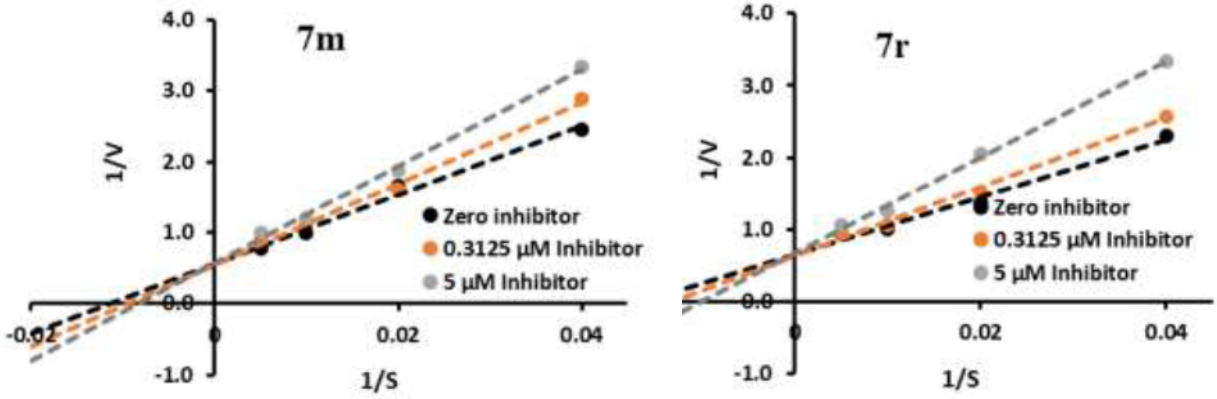

Table 7.2. K_m, V_{max} and K_i values of **7m** and **7r** retrieved from the PL enzyme kinetics.

Code	K_m (apparent) at different concentration (µM)			V_{max} (µM/min)	K_i µM	Nature of inhibition
	0 µM	0.3125 µM	5 µM			
7m	62.188	77.492	100.711	1.312	1.483	Competitive
7r	87.833	105.134	121.448	1.803	2.924	Competitive

Based on the *in-vitro* PL inhibition assay, a preliminary structure-activity relationship of the screened analogues was deduced and the obtained SAR was similar to the previous series. As represented in **Fig. 7.5**, presence of denser aromatic functionalities on the imidic nitrogen of TZD attached with additional carbon linker resulted in the enhancement of PL inhibition. Phenyl substitution of the **7d** with an indole scaffold resulted in the formation

7m, that exhibited a potential PL inhibition (IC_{50} = 4.22 µM) than the earlier analogue (IC_{50} = 5.01 µM). Further, substitution of aromatic functionalities on the indole scaffold significantly increased the PL inhibition activity of analogues in comparison to the simple alkyl/ unsubstituted counterparts, that was similar to the previous series. Apart from this, the incorporation of the geranyl/ unsaturated alkyl groups resulted in an enhanced PL inhibition. **7r** with a geranyl group resulted a IC_{50} value of 2.67 µM, while prenyl substituted analogue (**7q**) resulted in IC_{50} value of 4.52 µM. Prenyl substituted analogues exerted comparatively slightly lesser activity than the benzyl substituted analogues. It is noteworthy that the enhancement of aromatic density *via.* attachment of benzyloxy substituent on indole (4,5 and 7 positions) resulted in the lowering of PL inhibition. 4 and 5 benzyloxy substitutions on indole scaffold resulted in a slight reduction in PL inhibitory potential, while 7-benzyloxy substitution resulted in greater reduction in the PL inhibitory potential when compared with **7r**.

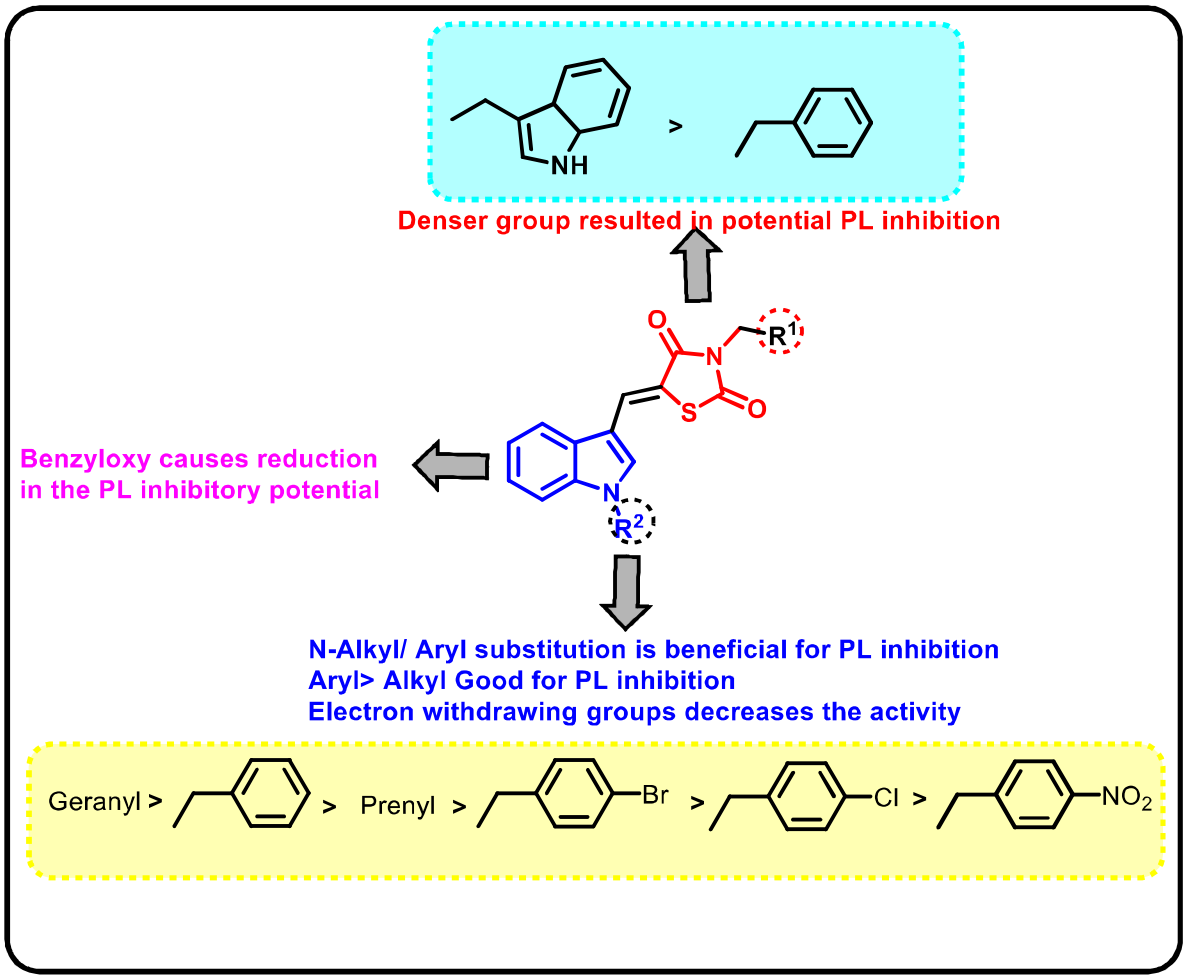

Fig. 7.5. Structure–activity relationship of synthesized Indole-TZD hybrid analogues (**7a**-**7u**)

7.4. Fluorescence Quenching Measurements with PL

The effects of the synthesized analogues (**7m** and **7r**) on the fluorescence quenching of PL were evaluated (See chapter 5) and the results are depicted in **Fig. 7.6** and **Table 7.3**. The screened analogues exerted a concentration dependant quenching effect on the PL fluorescence.

As represented in **Table 7.3**, an inverse correlation between the K_{sv} and temperature was obtained, that suggested the quenching effects on the PL may be mainly attributed to static quenching. Furthermore, K_q values were in the range of 39 to 81 (10^{10} M^{-1} s^{-1}) supporting the static mechanism-based quenching, wherein both analogues formed a complex with PL.

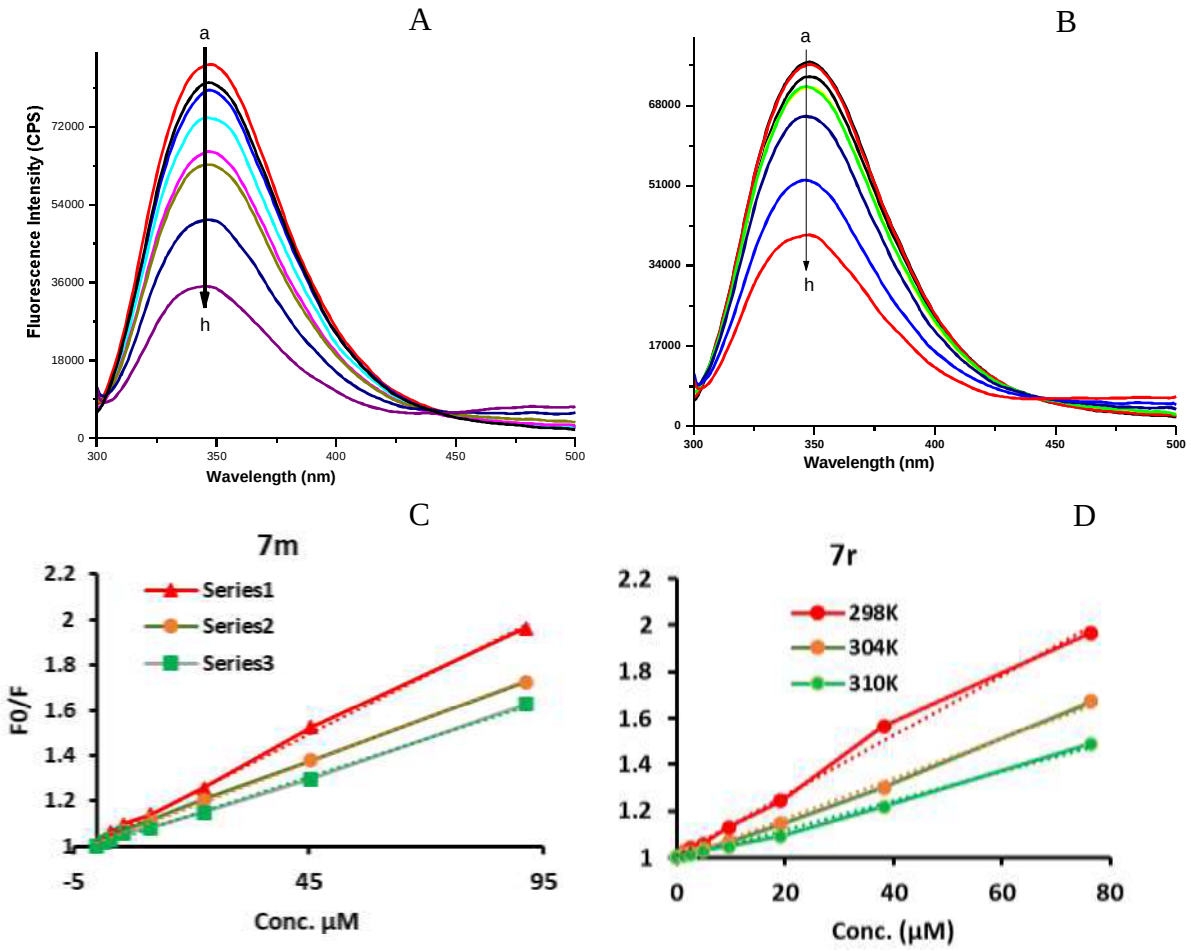

Fig. 7.6. (A), (B) The fluorescence spectra of PL in the presence of **7m** and **7r** at various concentrations (pH 7.4, a to h in increasing concentrations); (C), (D) Stern−Volmer plots for the quenching of **7m** and **7r** on the PL

Table 7.3. Bimolecular quenching constant (K_q), binding constant (K_b) and the number of binding sites (n) at different temperatures for **7m** and **7r**

#	T (K)	K_{SV} ($\times 10^4$ M^{-1})	K_q ($\times 10^{10}$ M^{-1} s^{-1})	R^2	K_b ($\times 10^4$ M^{-1} s^{-1})	n	R^2
7m	298	1.04	65.41	0.9977	2.51	0.757	0.9927
	304	0.78	49.06	0.9983	1.55	0.841	0.9986
	310	0.67	42.14	0.9977	1.24	0.836	0.9938
7r	298	1.29	81.13	0.9938	1.62	0.9386	0.9934
	304	0.87	54.72	0.9962	1.05	0.9135	0.9855
	310	0.63	39.62	0.994	0.48	1.046	0.9952

Based on the modified Stern-Volmer equation, number of binding sites and binding constant were calculated, that further supported the inhibitory potential of these analogues. The values of "*n*" at the corresponding temperature were in the range of 0.757 to 1.046, indicating that these analogues bind to the active site, *via* a competitive inhibition mode as deduced from the enzyme inhibition kinetics. Moreover, strong binding forces of these analogues with PL have been identified from the binding constant (K_b) values, that were in the range 0.48 to 2.51 ($\times 10^4$ M^{-1} s^{-1})

7.5. Molecular docking and Dynamics

A total of 21 indole-TZD hybrid analogues were subjected to molecular docking studies, while the most active analogues **7m** and **7r** were also subjected to MD simulations. The MolDock scores and the various interactions exhibited by the hybrid analogues are summarized in **Fig. 7.7** and **Table 7.4.** The MolDock scores of the analogues exhibited significant correlation to their PL inhibitory activity (Pearson's $r = 0.8355$, $p < 0.05$) and these activities were exerted *via* various interactions such as hydrogen bonding, π- π, π-sulfur, and π-cation interactions etc. The most active analogue **7r** from the series possessed a top docking score of -163.169 kcal/mol, while **7m**, the second most active in the series, exhibited a MolDock score of -138.384 kcal/mol. Majority of the molecules exhibited a consistent H-bond interaction with Gly 76, Phe77, His 151 and Ser152. Apart from this π-π interactions with lid domain amino acids were prominent in all of the synthesized analogues.

Further, the *N*-geranyl substitution resulted in the overall hydrophobicity of analogues that in turn resulted in the additional interactions with various amino acids. For instance, in the

case of analogue **7r**, the geranyl extension resulted in additional **π** interactions with Phe 77, Ile 78, Phe 215 and Ala 260 (**Fig. 7.7**). The formation of these additional **π** interactions might be attributed to the amplification of the lid domain interactions thereby resulting in the increased PL inhibitory activity. Further, molecular modelling study revealed that the benzyl substituted analogue (**7m**) exerted a 3.09 Å distance from the reactive carbonyl group (**Fig. 7.8**). Nevertheless, replacement of phenyl substituent to geranyl (**7r**) resulted in the reduction of interaction distance to 2.77 Å. Accordingly, an increase in the PL inhibitory activity was clearly visible (IC_{50} = 4.22 to 2.67 µM).

The overall hydrophobicity of indole functionality can be further improved by the additional substitutions in the 4 to 7 positions of the basic indole scaffold. Previously, the increase of hydrophobicity of indole scaffold *viz* various benzyloxy substituents in the PL inhibition have been explored. Thus, an attempt was made, wherein numerous benzyloxy functionalities were incorporated to the most active analogue, i.e., **7r**, that resulted in analogues **7s** to **7u**.

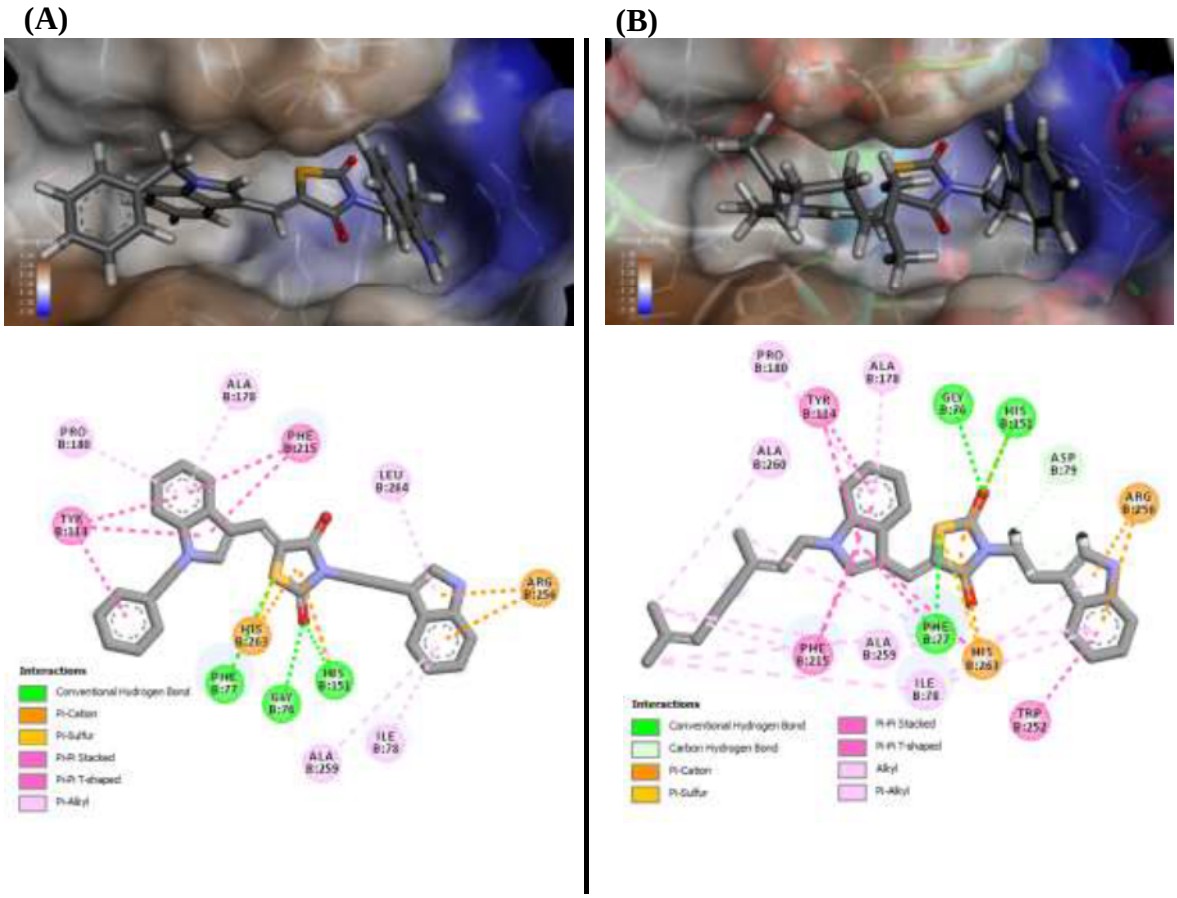

Fig. 7.7. Binding pose and 2D interaction diagram of **7m** (A) and **7r** (B) in the active site of PL (1LPB)

However, further substitution in the indole by additional benzyloxy substituents exerted varied activities. **7s** (4-benzyloxy) and **7t** (5-benzyloxy) exhibited a comparable activity to the parent analogue **7r**, while **7u** (7-benzyloxy) resulted in a greater reduction in the PL inhibitory activity (**Table 7.1**). This was also correlated with their interaction distance wherein **7s** and **7t** exhibited a similar interaction distance from the Ser152, as observed with **7r**, while **7u** revealed a larger interaction distance from Ser 152 (**Fig. 7.8**). These data clearly indicate that the further substitution of indole scaffold with larger functionalities exerted an inverse correlation with PL inhibitory potential and steric hindrance might be the probable reason for the lowering of PL inhibition.

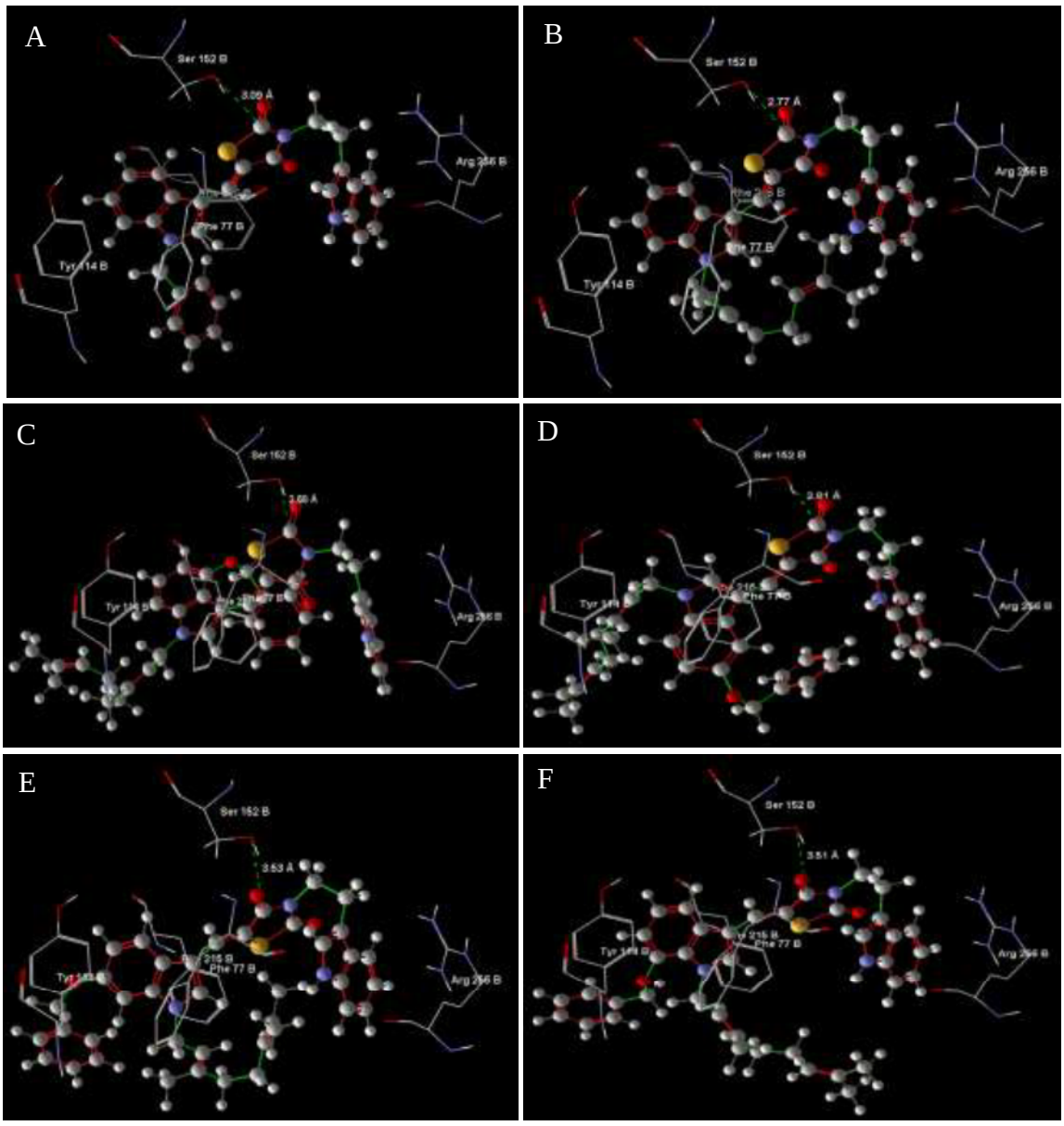

Fig. 7.8. 2D docking poses of **7m** (A), **7r** (B), **7s** (C), **7t** (D), **7u** (E) highlighting the distance of the reactive carbonyl from Ser 152; (F)- 6 methoxy substituted analogue.

Table 7.4. Mol Dock scores (in kcal/ mol) and the interaction summary of the synthesized analogues **(7a- 7u)** with the human PL active site of 1LPB

#	Mol Dock Score	H-bond	π-π interaction	π-cation	Alkyl/π-alkyl	π-Sulfur
7a	-97.906	His-151	Phe-77, Phe-215	His-151, His-263	Ala-178, Arg-256, Ala-259, Ala-260, Leu-264	His-263
7b	-99.576	Phe-77, Gly-76, His-151	Phe-77, Phe-215	His-151, His-263	Arg-256, Ala-259, Ala-260, Leu-264	His-263
7c	-107.087	Phe-77, Gly-76, His-151, Ser-152	Phe-77, Phe-215	His-151, His-263	Pro-180, Ile-209, Arg-256, Leu-264	His-263
7d	-130.610	Phe-77, His-151, Ser-152	Phe-77	His-151, His-263	Ile-78, Pro-180	His-263
7e	-113.874	Ser-152	Phe-77, Phe-215	His-151, His-263	Ile-78, Pro-180, Ala-259	His-263
7f	-97.079	Gly-76, His-151	Phe-77, Tyr-114, Phe-215	His-151, His-263	Ala-178, Pro-180, Arg-256, Ala-259, Ala-260, Leu-264	His-263
7g	-113.908	Ser-152	Phe-77, Tyr-114, Phe-215	His-151, His-263	Ile-78, Pro-180, Ile-209, Ala-259, Ala-260	His-263
7h	-130.632	Phe-77, His-151, Ser-152	Phe-77, Phe-215	Asp-79, His-151, Arg-256, His-263	Ile-78, Tyr-114, Pro-180, Cys-181, Ile-209	His-263
7i	-135.510	His-151, Ser-152	Phe-77, Phe-215	Asp-79, His-151, Arg-256, His-263	Ile-78, Tyr-114, Pro-180, Ile-209	His-263
7j	-105.592	Phe-77, Gly-76, His-151, Arg-256	Phe-77	Asp-79, His-151, Arg-256	Ile-78, Ala-178, Pro-180, Ala-259, Ala-260, Leu-264	His-151, His-263
7k	-109.190		Phe-77, Tyr-114	His-151, His-263	Pro-180, Ile-209, Ala-260, Leu-264	Phe-77
7l	-110.946	Phe-77, Gly-76, His-151	Phe-77, Tyr-114, Phe-215	Asp-79, Arg-256, His-263	Ile-78, Ala-178, Pro-180, Ile-209, Phe-215, Ala-259, Leu-264	His-263

… Contd

#	Mol Dock Score	H-bond	π-π interaction	π-cation	Alkyl/π-alkyl	π-Sulfur
7m	-138.384	Gly-76, Phe-77, His-151	Tyr-114, Phe-215	Arg-256, His-263	Ile-78, Pro-180, Ala-178, Ile-209, Ala-259, Leu-264	Phe-77
7n	-130.980	--	Tyr-114, Phe-215	Arg-256, His-263	Ala-178, Pro-180, Ile-209, Trp-252, Ala-259, Ala-260, Leu-264	
7o	-123.371	--	Tyr-114, Phe-215	Arg-256, His-263	Ala-178, Pro-180, Ile-209, Trp-252, Ala-259, Ala-260, Leu-264	
7p	-116.448	Arg-256	Phe-77, Tyr-114	Asp-79, His-151, Arg-256, His-263	Ile-78, Ala-178, Pro-180, Ile-209, Phe-215, Ala-259, Leu-264	Phe-77
7q	-144.884	Gly-76, Phe-77, His-151	Tyr-114, Phe-215, Trp-252	Asp-79, Arg-256, His-263	Ile-78, Ala-178, Pro-180, Ala-259, Leu-264	His-263
7r	-163.169	Gly-76, Phe-77, His-151	Tyr-114, Phe-215	Arg-256, His-263	Ile-78, Pro-180, Ile-209, Ala-260, Leu-264	His-263
7s	-138.952	Gly-76, Phe-77, His-151	Phe-77, Tyr-114	Asp-79, Arg-256, His-263	Ile-78, Pro-180, Ile-209, Leu-264	Phe-77, His-263
7t	-123.118	Gly-76, Phe-77, His-151	Phe-77, Tyr-114	Asp-79, Arg-256, His-263	Ile-78, Pro-180, Ile-209, Phe-215, Ala-259, Ala-260, Leu-264	His-263
7u	-97.906	Ser-152, Cys-181	Phe-77, Tyr-114	His-151, His-263	Ile-78, Ile-209, Trp-252, Arg-256, Ala-260	Cys-181
Orlistat	-107.750	Phe-77, Ser 152, His 263	Tyr-114, Trp-252	--	Arg-256, Ala-259,	--

A 20 ns MD simulation was performed for **7m** and **7r** in complex with PL and the respective ligand RMSD are represented in **Fig. 7.9.** Analogue **7m** exhibited a rapid flotation at 2.5 sec and further it acquired a comparatively stable conformation during the MD run, with a maximum deviation of 0.8 nm, observed around 8 ns. On the other hand, **7r** remained comparatively stable during the entire MD simulation. A maximum RMSD of 0.4 nm, observed around 10 ns. Furthermore, a stable radius of gyration indicated the compactness of the 1LPB during the MD run with test analogues.

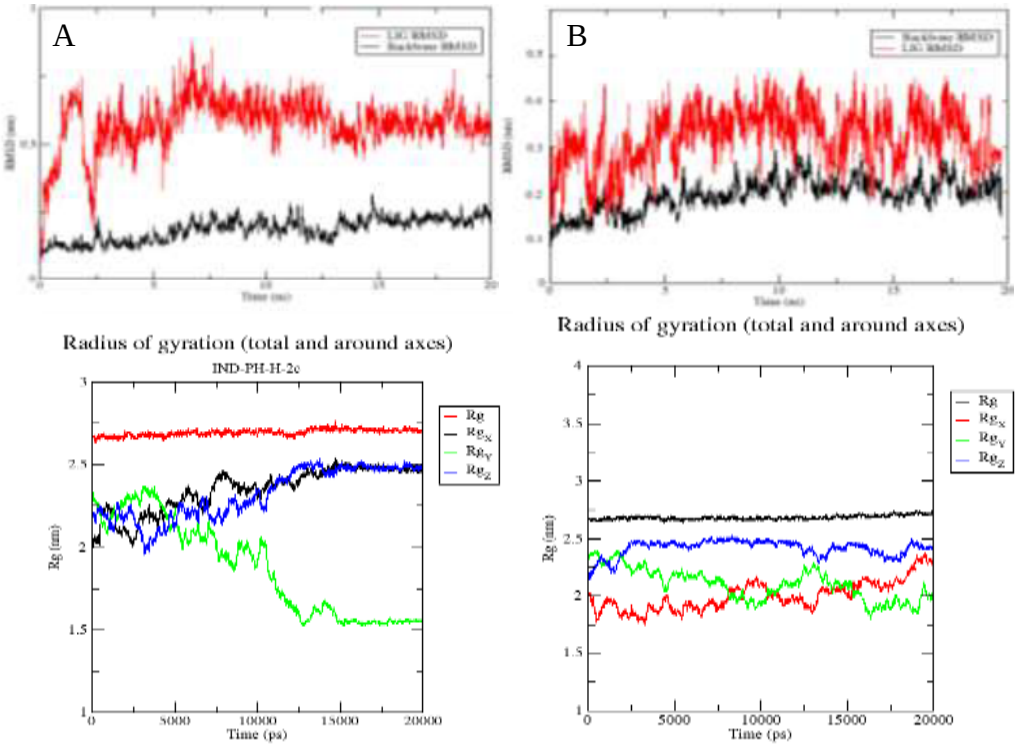

Fig. 7.9. RMSD of ligands and radius of gyrations retrieved from 20 ns MD simulations of the PL-ligand complexes (A)-**7m** and (B)-**7r**

The obtained interactions of these analogues with 1LPB complex during 20 ns of MD simulation are summarised in **Table 7.5.** The ligand analogues exhibited numerous interactions such as H bonding, π-π, π-alkyl and π-sulfur interactions etc. Both analogues exhibited a H bond interaction with Phe 77, Asp 79. It also resulted in a consistent π-π interaction with the lid domain amino acids (Phe 77, Tyr 114, Phe 215 etc.). Additionally, a prominent π-cation interaction with Arg 256 was also observed. Apart from this, numerous π-alkyl interactions (with Ile 78, Ala 178, Pro 180, Ile 209, Arg 256) were also generated during the MD run. Nevertheless, Phe 77, His 151, His 263 were also involved in the formation of π-sulfur interactions.

Table 7.5. Various interactions exhibited by **7m** and **7r** with PL during the 20 ns MD run

Time (ns)	H Bond	π-π Interaction	π-cation Interaction	π -alkyl	π -Sulfur
7m					
0	Phe-77	Phe-77, Tyr-114, Phe-215	--	Ile-78, Pro-180, Arg-256	Phe-77, His-263
2	--	Phe-77, Tyr-114, Phe-215	--	Ile-78, Ala-178, Pro-180, Ala-259	Phe-77
4	--	Tyr-114, Phe-215, Ala-259	--	Ala-178, Pro-180, Ala-260	--
6	Asp-79	Phe-77, Tyr-114, Phe-215	Arg-256	Ile-78, Ala-178, Pro-180, Ile-209, Arg-256	--
8	Asp-79	Phe-77, Phe-215, Trp-252	Arg-256	Ile-78, Ala-178, Pro-180, Arg-256	--
10	Asp-79	Phe-77, Tyr-114, Phe-215	Arg-256	Ile-78. Ala-178	--
12	Asp-79	Phe-77, Phe-215, Trp-252	Arg-256	Ile-78, Leu-153, Ala-178, Pro-180, Arg-256, Ala-259	Phe-77
14	Asp-79	Tyr-114, Phe-215	Arg-256	Ala-178, Pro-180, Arg-256, Ala-259,	Phe-77
16	--	Phe-77, Tyr-114, Phe-215	Arg-256	Ile-78, Ala-178, Pro-180, Arg-256, Ala-259, Ala-260, Leu-264	--
18	Asp-79	Tyr-114, Phe-215	Arg-256	Ile-78, Ala-178, Arg-256	Phe-77
20	Asp-79	Phe-77, Tyr-114	--	Ile-78, Ala-178, Ala-259	--
7r					
0	--	Phe-77, Tyr-114, Phe-215, Trp-252	--	Ile-78, Ala-178, Pro-180, Leu-213, Arg-256, Ala-259	His-151, His-263
2	Phe-77	Phe-77, Tyr-114, Phe-215, Trp-252	Arg-256	Tyr-114, Ala-178, Pro-180, Ile-209, Arg-256, Ala-259	His-151
4	--	Ile-78, His-263	Asp-205	Phe-77, Tyr-114, Ala-178, Pro-180, Ile-209, Phe-215, Ala-259	His-151
6	Phe-77	His-263	Arg-256	Phe-77, Tyr-114, Ala-178, Pro-180, Arg-256, Ala-259	His-151, His-263
8	Phe-77	Phe-77, Tyr-114, Phe-215, Thr-255, His-263	Arg-256	Ala-178, Pro-180, Arg-256, Ala-259	His-151, His-263
10	Phe-77	Tyr-114, His-263	--	Ala-178, Pro-180, Arg-256, Ala-259	His-151, His-263
12	--	Trp-252	Arg-256	Ile-78, Tyr-114, Ala-178, Pro-180, Phe-215, Arg-256, Ala-259	His-151, His-263
14	--	Phe-77, Phe-215	Arg-256	Tyr-114, Ala-178, Pro-180, Phe-215, Arg-256, Ala-259	Phe-77, His-263
16	--	Phe-77, Phe-215, Thr-255	--	Tyr-114, Ala-178, Pro-180, Arg-256, Ala-259	Phe-77, His-151, His-263
18	Asp-79	Phe-215, Trp-252	Arg-256	Tyr-114, Ala-178, Arg-256, Ala-259	His-151, His-263
20	--	Phe-77	--	Ala-178, Pro-180, Arg-256, Ala-259, Leu-264	His-151, Ser-152, His-263

In conclusion, the present chapter was aimed to maintain/enhance the π-cation interaction of Arg256 with the aromatic functionality and to enhance the hydrophobicity of the hybrid analogues. Incorporation of additional carbon linker between the imidic nitrogen of TZD and aromatic functionalities resulted in an increased PL inhibition (**7d**; IC_{50} = 5.01 µM), that preferably was due to the increment in the Arg 256 interaction. Further, modification of the simple aromatic functionalities into heteroaromatic system (indole) resulted in the further enhancement of PL inhibition (**7m**; IC_{50} = 4.22 µM). Hydrophobicity of hybrid analogues was enhanced by the incorporation of prenyl/geranyl substituents, wherein geranyl substituents resulted in the potent activity (**7r**; IC_{50} = 2.67 µM), comparable to that of orlistat (IC_{50} = 0.86 µM).

References

[1] M.E. Lowe, Pancreatic triglyceride lipase and colipase: Insights into dietary fat digestion, Gastroenterology. 107 (1994) 1524–1536.

[2] S.N.C. Sridhar, D. Bhurta, D. Kantiwal, G. George, V. Monga, A.T. Paul, Design, synthesis, biological evaluation and molecular modelling studies of novel diaryl substituted pyrazolyl thiazolidinediones as potent pancreatic lipase inhibitors, Bioorg. Med. Chem. Lett. 27 (2017) 3749–3754.

[3] R.B. Birari, S. Gupta, C.G. Mohan, K.K. Bhutani, Antiobesity and lipid lowering effects of *Glycyrrhiza* chalcones: Experimental and computational studies, Phytomedicine. 18 (2011) 795–801.

[4] J.C. Ma, D.A. Dougherty, The cation-π interaction, Chem. Rev. 97 (1997) 1303–1324.

[5] M.T. Ha, M.H. Tran, K.J. Ah, K.-J. Jo, J. Kim, W.D. Kim, W.J. Cheon, M.H. Woo, S.H. Ryu, B.S. Min, Potential pancreatic lipase inhibitory activity of phenolic constituents from the root bark of *Morus alba* L., Bioorg. Med. Chem. Lett. 26 (2016) 2788–2794.

[6] S.N.C. Sridhar, G. George, A. Verma, A.T. Paul, Natural Products-Based Pancreatic Lipase Inhibitors for Obesity Treatment, in: Nat. Bio-Active Compd., Springer, 2019: pp. 149–191.

[7] S.N.C. Sridhar, G. Ginson, P.O.V. Reddy, M.P. Tantak, D. Kumar, A.T. Paul, Synthesis, evaluation and molecular modelling studies of 2-(carbazol-3-yl)-2-oxoacetamide analogues as a new class of potential pancreatic lipase inhibitors, Bioorg. Med. Chem. 25 (2017) 609–620.

[8] S.N.C. Sridhar, S. Palawat, A.T. Paul, Design, synthesis, biological evaluation and molecular modelling studies of conophylline inspired novel indolyl oxoacetamides as potent pancreatic lipase inhibitors, New J. Chem. 44 (2020) 12355–12369.

[9] K. Tilekar, N. Upadhyay, N. Jänsch, M. Schweipert, P. Mrowka, F.J. Meyer-Almes, C.S. Ramaa, Discovery of 5-naphthylidene-2,4-thiazolidinedione derivatives as selective HDAC8 inhibitors and evaluation of their cytotoxic effects in leukemic cell lines, Bioorg. Chem. 95 (2020) 103522.

[10] Y. Momose, K. Meguro, H. Ikeda, C. HatanakaA, S. Oi, T. Sohda, Studies on antidiabetic agents. X. Synthesis and biological activities of pioglitazone and related compounds., Chem. Pharm. Bull. 39 (1991) 1440–1445.

[11] G. George, P.S. Dileep, A.T. Paul, Development and validation of a new HPTLC-HRMS method for the quantification of a potent pancreatic lipase inhibitory lead Echitamine from *Alstonia scholaris*, Nat. Prod. Res. (2019) 1–5.

[12] B.T. Burlingham, T.S. Widlanski, An intuitive look at the relationship of K_i and IC_{50}: A more general use for the Dixon plot, J. Chem. Educ. 80 (2003) 214-217.